Synchrotron-based far infrared study of the rotation-vibration-inversion spectrum of silacyclobutane below 500 cm^{-1}: The ν_{29} and ν_{30} bands

Ziqiu Chen and Jennifer van Wijngaarden*

Department of Chemistry, University of Manitoba, Winnipeg Manitoba, R3T 2N2 Canada

*Corresponding author

Email: vanwijng@cc.umanitoba.ca

Phone: (204)474-8379

Fax: (204)474-7608

Abstract

Fourier transform spectra of the four-membered heterocycle silacyclobutane (c-C_3H_8Si) were recorded in the far infrared region from 100-500 cm^{-1} with a maximum resolution of 0.000959 cm^{-1} using synchrotron radiation from the Canadian Light Source. The two fundamental bands observed in this region correspond to motions best described as the out-of-plane modes related to ring puckering (ν_{30}) at ~158 cm^{-1} and SiH_2 rocking (ν_{29}) at ~410 cm^{-1}. Both bands exhibit complex, dense spectral patterns that arise from ring inversion tunneling of the puckered SCB ring through a planar (C_{2v}) intermediate configuration. Analysis of these patterns revealed rotation-vibration transitions between states of the same inversion symmetry as well as rotation-vibration-inversion transitions that connect states of different inversion symmetry. Infrared ground state combination differences from 1871 pairs of P and R branch transitions were used to accurately determine the spectroscopic parameters for the tunneling-doubled ground state based on a broad range of quantum levels. With the ground state energy levels well-determined, 8255 infrared transitions were assigned and analyzed to derive the band centers, rotational and centrifugal distortion constants for the inversion split ν_{29} and ν_{30} vibrational states. Comparison with the band centers predicted via DFT (B3LYP) and MP2 calculations [6-311++G(2d,2p)] suggests that anharmonic corrections found via perturbation theory typically agree within 2% when compared with the observed spectrum of SCB.

KEYWORDS: rovibrational spectroscopy; ring inversion; ring puckering; synchrotron; silacyclobutane; computation

1. Introduction

Over the past few years, mono- and di-silacyclobutanes along with their methyl-substituted derivatives, have been the subject of renewed theoretical and experimental interest as potential precursors for the synthesis of organosilicon materials such as silicon carbide films.[1,2,3,4] Compared with other compounds, a principal advantage of the silacyclobutanes for SiC film deposition is that the high ring strain facilitates their decomposition at lower temperatures.[5] As the stability and reactivity of this family of compounds is inherently linked to their ring strain energy, a systematic investigation of molecular properties as a function of substituent is of great practical and theoretical interest. High resolution spectroscopy provides a detailed molecular fingerprint of individual compounds that is sensitive to the underlying potential energy surface and thus offers great promise is this regard.

The relationship between the structure and the low frequency spectra of small heterocycles has been the subject of numerous reviews.[6,7,8] The equilibrium geometry of silacyclobutane (SCB), for example, has a puckered ring backbone with a barrier to planarity of ~440 cm^{-1} along the ring puckering coordinate as shown in Figure 1.[9,10] This potential form gives rise to ring inversion tunneling splitting in the microwave spectrum and irregularly spaced hotbands in the far infrared spectrum of the lowest frequency vibration. The analogous potential function in oxetane (c-C_3H_6O), by contrast, has a barrier of only ~35 cm^{-1} which lies below the ground vibrational state.[11,12,13] This results in an equilibrium structure in which the heavy atoms of the ring are quasiplanar. No tunneling features were observed in the microwave or far infrared spectra and the hotbands of the ring puckering vibration are more regularly patterned.[14,15]

Although such four-membered rings have been under spectroscopic scrutiny for half a century, the development of higher resolution techniques opens new possibilities to characterize

their unique spectroscopic signatures with an unprecedented level of detail. For example, we recently reported the Fourier transform microwave (FTMW) spectrum of SCB and resolved the ring inversion tunneling splitting in the *a*-type spectrum of the ground state for the first time.[16] This splitting was only ~10 kHz for the lowest transitions and thus inaccessible in earlier microwave studies.[10] Through measurement of *c*-type transitions crossing between states of different inversion symmetry (0^+ and 0^-), the energy level difference caused by ring inversion in the ground vibrational state was determined to be 75.7260(19) MHz. The geometric parameters of the ring backbone were derived using isotopic substitution (^{13}C, ^{29}Si, ^{30}Si) and the ring puckering angle (31.1(4)^o) in the ground state compares favourably with that reported via *ab initio* methods (34.5^o, MP2/cc-pVTZ)[17] and gas phase electron diffraction (33.5^o) experiments.[18]

The use of synchrotron far infrared radiation as a light source for vibrational spectroscopy is another technological advance that holds great promise for probing small molecules with very high resolution (better than 0.001 cm^{-1}).[19] The high photon flux of synchrotron radiation allows the study of low intensity spectral features as well as the use of narrow apertures to achieve the high resolution needed to unravel tunneling splittings and to characterize minor perturbations. Although SCB has been the subject of a number of infrared and Raman studies,[9,20,21] there are no rotationally-resolved studies to date. The most recent, comprehensive vibrational study of SCB was reported in 2008 and the observed spectra were compared with empirically-scaled DFT (B3LYP) level harmonic frequency calculations.[17] Based on these calculations, nine of the previously studied[21] fundamental bands were re-assigned. It was also determined that the out-of-plane CH_2 twisting and CH_2 wagging modes (not observed in ref 17) were predicted to lie at much lower frequencies (969 cm^{-1} and 1074 cm^{-1}) than in the original assignment (1255 cm^{-1} and 1343 cm^{-1}). Similar discrepancies are not uncommon in the

literature and while computational techniques are now playing a larger role in vibrational assignments, rotationally-resolved spectra provide irrefutable, experimental evidence for correcting such mis-assignments.[22]

This article describes the first rotationally-resolved vibrational investigation of SCB and focuses on the region below 500 cm^{-1} using spectra recorded at the Canadian Light Source (CLS) synchrotron. The assignment of the dense spectral patterns of the ν_{29} SiH_2 rocking and the ν_{30} ring puckering motions at ~410 cm^{-1} and ~158 cm^{-1}, respectively reveals the presence of ring inversion tunneling in both vibrational modes. The successful analysis of the complex rotation-vibration and rotation-vibration-inversion spectra of these two lowest frequency bands with the aid of molecular symmetry group theory has provided a set of accurately determined spectroscopic constants for the ground, ν_{29} and ν_{30} excited vibrational states including a measure of the inversion tunneling splitting of the energies. The currently observed and previously reported infrared band centers are compared with predicted vibrational frequencies from new *ab initio* and DFT calculations that include anharmonic perturbation corrections.

2. Experimental details

As SCB is not commercially available, the sample was prepared by a one-step reduction[20] of 1,1-dichlorosilacyclobutane (GELEST, 97%). This precursor was mixed with $LiAlH_4$ in a 2:1 ratio in *n*-butyl ether for 24 h. The final product was distilled from the mixture at 110 °C using a dry ice/acetone-cooled receiving flask and verified by GC/MS.

The rovibrational spectra of SCB were collected at the CLS using synchrotron light as the source for a high resolution Fourier transform infrared (FTIR) spectrometer (Bruker IFS125HR). The low pressure gas sample was prepared by introducing vapour from the liquid sample into a

multipass gas cell (80 m absorption path length) from the synthesized liquid sample. The spectra of the ν_{29} and ν_{30} bands were recorded in two separate spectral windows as the required optical components have different operating ranges. For the ν_{29} band near 410 cm^{-1}, the spectrometer was outfitted with a 6 μm Mylar beamsplitter and a GeCu detector. A total of 528 interferograms were recorded at a resolution of 0.000959 cm^{-1} over 105 hours at a sample pressure of 448 mTorr. The spectrum of the lower intensity ν_{30} band centered around 158 cm^{-1} was collected at a higher pressure (1060 mTorr) with a 75 μm Mylar beamsplitter and a helium-cooled Si bolometer detector. The instrumental resolution was set at 0.001918 cm^{-1} to reflect the expected pressure broadening of transitions under these conditions and this allowed faster data collection for the 844 interferograms (84 hours).

The observed spectra were calibrated using transitions due to residual water vapour in the two spectral ranges which were compared to the reported frequencies of the ground state rotational transitions listed in the HITRAN database.[23] All observed H_2O transitions in the 158 cm^{-1} region were subsequently verified using the line list from the JPL catalog[24] which reported uncertainties in the ground state line positions of 0.0001 cm^{-1} or less. For the 410 cm^{-1} region, the transition frequencies could only be verified up to 330 cm^{-1} using the JPL catalog (also with uncertainties of better than 0.0001 cm^{-1}) and it was assumed that the remaining HITRAN data for the ground state was similarly reliable throughout the region of this band. Following calibration, the recorded frequencies of SCB in both spectral regions were determined to be accurate to within 0.0003 cm^{-1}.

3. Frequency calculations

The harmonic vibrational frequencies of SCB were calculated using Gaussian 03W[25] at the DFT/B3LYP and MP2 levels of theory with a 6-311++G(2d,2p) basis set following geometry optimization. Two sets of calculations were done such that the optimized geometry was constrained to either the C_s or C_{2v} (planar) point group as the latter symmetry helps identify the principal nature of the mode as in-plane or out-of-plane and provides convenient labels to group the transitions (A_1, A_2, B_1, B_2) for comparison with earlier studies.[17] Anharmonic corrections were subsequently determined via second order perturbation analysis in G03W as our previous work on β-propiolactone[26] showed that the anharmonic estimates were in better agreement with experimental results in this region. This result was achieved at a steep computational price, however, as the anharmonic calculations took nearly 100 times longer to complete at the DFT level and 75 times longer at the MP2 level. The calculated frequencies for SCB are listed in Table 1 along with descriptions of the corresponding motions. The band numbering follows that established by Al-Saadi and Laane[17] but the B_1 and B_2 vibrational symmetry labels are reversed for the C_{2v} case as we have chosen to define the plane of the SCB molecule as yz to allow direct correlation with the axis system under C_s symmetry. The latter has the y-axis passing through the Si atom and the symmetry plane bisecting the puckered ring is labelled xy.

4. Symmetry considerations

Although the ground state structure of SCB (shown in Figure 2) belongs to the C_s point group, the molecular symmetry group C_{2v} is used to account for the ring inversion tunneling between the two equivalent minima of the symmetric double well potential. This potential function has a barrier to planarity of 440 cm^{-1} (ref. 9,10) and the ground vibrational state is split

into two components (labelled as 0^+ and 0^- in Figure 1) where the superscript describes the symmetry of the inversion part of the wavefunction (B_1). The two far infrared bands observed in this study arise due to out-of-plane vibrations which are attributed to the ring puckering (ν_{30}) and SiH_2 rocking motions (ν_{29}). Under C_{2v} symmetry (with the ring in the yz plane), these correspond to the B_1 irreducible representation. Figure 3 shows the symmetries of the rotation-vibration-inversion energy levels involved for the two far infrared bands investigated in this work. These include the two ring inversion tunneling components of the ground vibrational state (0^+ and 0^-) and two analogous components of the ν_{29} or ν_{30} excited vibrational state (1^+ and 1^-) with their rotational sublevels labeled with K_aK_c quantum numbers as either even(e) or odd(o). By symmetry, allowed transitions are those such that the product of the symmetries of the wavefuction ($\Gamma_{rot}\times\Gamma_{vib}\times\Gamma_{inv}$) for each state must contain the totally symmetric (A_1) representation when combined with the symmetry of the space-fixed molecular dipole moment (A_2). This means that transitions occur between levels of A_1 and A_2 symmetry or B_1 and B_2 symmetry in Figure 3. Careful examination of the symmetry of the levels shows that there are four sets of allowed transitions for each band: two sets of *c*-type transitions ($0^+ \rightarrow 1^+$, $0^- \rightarrow 1^-$) (connecting states of the same inversion symmetry) and two sets of *a*-type transitions ($0^- \rightarrow 1^+$, $0^+ \rightarrow 1^-$) (connecting states of opposite inversion symmetry).

5. Spectral assignment and analysis

Initially, the observed rovibrational transitions in the ν_{29} and ν_{30} bands of SCB were assigned and fit separately using Watson's A-reduced Hamiltonian in I^r representation in Pickett's SPFIT program.[27] During this process, sets of ground state combination differences (GSCD) were collected so that the ground state parameters (0^+ and 0^-) could be determined in

isolation to remove any potential perturbation effects from excited states. Ultimately, the infrared transitions from both bands were merged in a global fit to obtain the final set of spectroscopic constants for the tunneling split ν_{29} and ν_{30} states. The various stages of the assignment and analysis are detailed below.

a) SiH_2 rocking (ν_{29}) mode

The ν_{29} band centered at ~410 cm^{-1} is attributed to SiH_2 rocking mode in SCB and the overall band contour is shown in Figure 4. No obvious patterns were observed in the initial visual inspection of the rotational structure of this band. To identify regularly spaced progressions, the most intense transitions between 390 and 430 cm^{-1} were used to construct a Loomis-Wood plot using a software add-in for Igor Pro.[28,29] As shown in Figure 5, P branch transitions of this band are grouped in such a way that those sharing common K_c quantum numbers but having different J values are arranged in a vertical series of K_c on the Loomis-Wood plot. These correspond to two sets of strong *c*-type progressions that connect vibrational levels of the same inversion symmetry ($0^+ \rightarrow \nu_{29}^+$ and $0^- \rightarrow \nu_{29}^-$). The observed pattern was then compared with the simulated rotation-vibration spectrum (based on the estimated band origins[17] and the ground state constants determined from the microwave study[16]), leading to the tentative assignment of a few of the strongest infrared transitions in this region. Ground state combination differences (GSCDs) derived from the microwave study confirmed the assignment of these *c*-type transitions. The simulated spectrum was then refined and the assignment process continued in an iterative manner until the strongest progressions were included.

After the assignment of the two sets of *c*-type transitions, obvious features remained unassigned in the Loomis-Wood plot shown in Figure 5. A second plot, given in Figure 6, shows

that these transitions arise from the tunneling-doubled *a*-type progressions that group transitions having common K_a but different J values. Note that the period (x-axis) depicted in this plot is about half that in Figure 5 to visualize the pattern of the two sets of *a*-type rotation-vibration-inversion transitions that connect levels of opposite inversion symmetry ($0^+ \rightarrow \nu_{29}^-$ and $0^- \rightarrow \nu_{29}^+$). A 0.6 cm^{-1} segment of the P branch spectrum is provided in Figure 7 and demonstrates the density of transitions in this region. Note that the unlabelled transitions were previously assigned to *c*-type progressions as described above. The assignment of the tunneling doubled *a*-type progressions followed the same procedure as for the *c*-type spectrum and ground state combination differences were closely tracked to avoid mis-assignment.

Overall, 6458 *a*-/*c*-type transitions from the ν_{29} band of SCB were assigned and fit: 3381 *c*-type transitions and 3077 *a*-type transitions. The quantum number coverage of the assigned lines is listed in Table 2. Analysis of the Q branch was attempted but the spectrum in this region was too dense to provide a convincing assignment.

b) Ring puckering (ν_{30}) mode

The ν_{30} band at ~158 cm^{-1} corresponds to the ring puckering motion of SCB. Initial inspection of the weak band contour shows a typical *c*-type envelope with a sharp Q branch feature as shown in Figure 8. A closer look revealed that transitions in the P and R branches had very low intensities resulting in S/N ratios of 5 at best even after 3.5 days of data collection. Furthermore, several regions of the P and R branches are obscured by hotband Q branches that were identified in the earlier low resolution study of SCB.[9] This, combined with the expected spectral congestion due to ring inversion tunneling, made the preliminary assignment of the ν_{30} band very challenging.

A Loomis-Wood plot was constructed to aid in the initial stages of the assignment as shown in Figure 9 for the R branch. Two sets of progressions were identified as the *c*-type transitions connection states of the same inversion symmetry ($0^+ \rightarrow \nu_{30}^+$ and $0^- \rightarrow \nu_{30}^-$) of SCB. The assignment scheme described above for the ν_{29} band was implemented and overall, 1797 *c*-type transitions were assigned between ~135 and ~181 cm^{-1}.The coverage of rotational levels is shown in Table 2. Although two sets of *a*-type rotation-vibration-inversion transitions are also allowed by symmetry, there were few unassigned transitions remaining after the *c*-type spectrum was fit as shown by the sparse Loomis-Wood plot in Figure 9. Thus, no *a*-type assignments were possible for this band as they were presumably buried in the noise of the spectrum. As the S/N scales with the square root of N (number of interferograms), it would have required 14 days of continuous measurement to double to S/N in this spectrum which was not feasible in the allocated beamtime and may not necessarily have provided further assignments.

c) Global analysis

The ground state spectroscopic constants were determined by fitting 1871 GSCDs collected during the assignment of the rovibrational transitions in the ν_{29} and ν_{30} bands. The resultant spectroscopic parameters of the two tunneling components of the ground state (0^+ and 0^-) are the same to within their 1σ uncertainties from the fit and are reported in Table 3. At this stage, all 8255 assigned rovibrational transitions from both bands were incorporated into a global fit using Watson's A-reduced Hamiltonian, I^r-representation in SPFIT[27] with the ground state spectroscopic constants held fixed to the values determined separately as described above. The rms error of the simultaneous two band fit was 0.000158 cm^{-1} and the resulting spectroscopic

constants and the energies of the various states relative to the 0^+ state are listed in Table 3. A complete list of all assigned rovibrational transitions is provided as Supplementary Material.[30]

6. Discussion

The observed vibrational spectra of the ν_{29} and ν_{30} bands of SCB are incredibly rich in detail due to the presence of ring inversion tunneling. This leads to a doubling of the rotation-vibration transitions (split on the order of 0.16 cm^{-1} in the ν_{29} band and 0.26 cm^{-1} in the ν_{30} band) and furthermore leads to the observation of two additional sets of transitions due to rotation-vibration-inversion involving these states in the ν_{29} band. The previous spectroscopic work on SCB proved invaluable in the analysis of the complex, densely packed far infrared spectra of these two bands. The reported microwave parameters provided initial estimates of GSCDs for confirming the preliminary assignments as well as approximate values of the energy gap due to ring inversion in both the ground state and excited ring puckering states of SCB.[10,16] Once the initial patterns in the far infrared spectrum were identified, a more extensive set of GSCDs were collected during the remaining assignment process. The final set of values included rotational energy levels up to J=52 and K_a=40 which ultimately provided a more accurate description of the 0^+ and 0^- states. The ground state spectroscopic parameters determined in the present study are compared with those derived solely from the microwave spectrum in Table 4. While the rotational constants are in fair agreement, the centrifugal distortion constants are less consistent. This is due to the fact that the microwave data set includes only 26 transitions with maximum J and K_a of 3. The microwave data was subsequently re-analyzed using the δ_J and δ_K values determined using the GSCDs from the far infrared spectra. As shown in the Table 4, this leads to

a more consistent set of centrifugal distortion constants and suggests that the parameters in the microwave study should be viewed as effective constants rather than physically meaningful.

With the ground state parameters of SCB well-determined via analysis of GSCDs, it was possible to fit over eight thousand infrared transitions involving rotational levels with J values up to 52 with a remarkably low rms error (0.000 158 cm^{-1}). The resulting parameters, shown in Table 3, are consistent in sign and magnitude across all states. Furthermore, this model Hamiltonian accounts for all observed P and R branch transitions of reasonable intensity in this spectral region. Although additional parameters related to interactions between the inversion doubled states were tested, the data was not sensitive to these extra terms.

The band origins of the ν_{29} ($0^+ \rightarrow \nu_{29}^+$ at 410.037649(15) cm^{-1} and $0^- \rightarrow \nu_{29}^-$ at 410.208815(22) cm^{-1}) and ν_{30} (ν_{30}^+ = 158.121851(8) cm^{-1} and ν_{30}^- = 158.384670(14) cm^{-1}) *c*-type modes of SCB were accurately determined for the first time. Using the observed *a*-type transitions that connect states of different inversion symmetry (+ → −, − → +), the relative ordering of the inversion components in the ground and ν_{29} excited vibrational states was unambiguously determined. The splitting of the energy levels of the SiH_2 rocking excited state was found to be 0.173831(30) cm^{-1} which is 70 times larger than the inversion splitting in the ground state of SCB (0.002665(6) cm^{-1}). The greater energy gap accounts for the observed differences in the rotational constants of these states in Table 3. The ground state parameters, for example, agree to within the 1σ uncertainty of the constants from the fit of the 0^+ and 0^- states whereas the rotational constants for the ν_{29}^+ and ν_{29}^- states differ by up to 1000 times the 1σ the uncertainty of the parameters.

As the ν_{30} band of SCB had only 5% the intensity of the neighboring ν_{29} band, the *a*-type transitions connecting states of different inversion symmetry were not observed and thus there

was no direct information about the ordering of the ν_{30}^{+} and ν_{30}^{-} states. As the ground state constants are the same to within their 1σ uncertainties, the upper state label is somewhat unclear if the two sets of *c*-type transitions are treated in isolation. Fortunately, Pringle reported room temperature microwave data[10] which included rotational transitions in the excited ring puckering states which could be used to confirm the ordering of the tunneling components as listed in Table 3. The splitting of the energy levels in the ring puckering excited state was determined to be 0.265484(16) cm^{-1} which is within 2% of Pringle's value of 0.25994 (23) cm^{-1}. This gap is more than two orders of magnitude larger than in the ground state and the subsequent large differences in the rotational constants were need to verify the ordering of the ν_{30}^{+} and ν_{30}^{-} states in comparison with Pringle's work. Of course, neither this study nor the prior microwave work successfully observed transitions that cross between the ν_{30}^{+} and ν_{30}^{-} tunneling states which would provide a direct measurement of this gap.

The band origins determined in this work (~410.0 cm^{-1} and ~158.1 cm^{-1} for the + states) are in close agreement with previous low resolution studies (~409 cm^{-1} and 157.8 cm^{-1})[9,17] of the SiH_2 and ring puckering frequencies, respectively. The experimental values for all fundamental vibrations of SCB reported by Al-Saadi and Laane[17] are given in Table 1 along with the results from the DFT(B3LYP) and MP2 level calculations (6-311++G(2d2p)) that include anharmonic corrections that were determined in the present work. The empirically-scaled frequencies reported in an earlier DFT(B3LYP/cc-pVTZ) study have also been included for comparison.[17] In general, the closest agreement comes from the DFT calculations based on C_s symmetry that include either anharmonic or scaling corrections as most match the corresponding experimental frequency within 2%. The anharmonic corrections perform marginally better in that they more closely predict ten of the fundamental band origins (as opposed to six for the scaled harmonic

calculations). There were several cases in which they provided similar levels of agreement but this may be coincidental and came at a steep computational cost as the anharmonic calculations took 100 times longer to run. On the other hand, the values of the scaling factors used in Ref. 17 are not reported in that study so it is not possible to gauge their applicability to other molecules.

Interestingly, the calculations in which C_{2v} symmetry was forced provide reasonable results for most bands above 900 cm^{-1} and the higher symmetry group was useful for categorizing the modes using C_{2v} labels (as needed to account for the ring inversion). Of course, the planar C_{2v} structure does not correspond to a minimum on the potential energy surface so these results should be treated with caution as is evidenced by the appearance of an imaginary number in Table 1 for the ring puckering frequency.

Finally, the mode with the poorest agreement with theory in Table 1 is the low energy ring puckering vibration of SCB which is underestimated by 8-20% using the various computational methods. This is perhaps not surprising as the ring puckering potential is known to be quite anharmonic as shown in Figure 1. In fact, efforts to model the barrier to planarity produced values ranging from 49-559 cm^{-1} when different basis sets and levels of theory were employed.[17] This suggests that empirical scaling factors and generic corrections to harmonic frequencies are insufficient for modeling such vibrations and that more extensive theoretical treatment is needed. This modeling should extend beyond predictions of band centers to include the effects of tunneling and other types of interactions that can now be elucidated using modern spectroscopic techniques as demonstrated here for the SCB molecule.

7. Summary

This article reports the first high resolution infrared spectroscopic investigation of the two lowest frequency modes of SCB using data recorded between 100 and 500 cm^{-1} at the Canadian Light Source synchrotron. The spectra are complicated by the presence of ring inversion which leads to tunneling-doubled rotation-vibration transitions as well as tunneling-doubled rotation-vibration-inversion transitions. The spectroscopic constants describing the ground state and the excited vibrational states corresponding to SiH_2 rocking (ν_{29}) and ring puckering (ν_{30}) motion of this highly fluxional molecule have been accurately determined for the first time. Through measurement of transitions that cross between states of opposite inversion symmetry and by comparison with previous microwave data, the energy difference and ordering of the tunneling states was also derived. This study provides the foundation for further investigation of SCB above 500 cm^{-1} which is now ongoing in our laboratory and provides information that can be used by researchers working to characterize the electronic structure of the silacylobutanes to better described the chemistry of organosilicon-based materials.[3]

Acknowledgements

JvW would like to extend her sincere thanks to W. C. Pringle for the many interesting discussions about SCB over the past few years and to B. Billinghurst for technical support at the Canadian Light Source. This research was funded by the Natural Sciences and Engineering Research Council of Canada (NSERC) through the Discovery Grants (JvW) and University Faculty Award (JvW) programs. We are grateful to the University of Manitoba for research fellowship support through the Faculty of Science and Faculty of Graduate Studies (ZC).

Table 1: Comparison of experimental band centers (Ref.17) of SCB and those calculated using DFT/B3LYP and MP2 theory (6-311++G(2d2p) in this work (with and without anharmonic corrections) and the empirically scaled DFT/B3LYP(cc-pVTZ) values from Ref. 17.

		expt	DFT C_s(anharm)	DFT C_s(harm)	MP2 C_s(anharm)	MP2 C_s(harm)	DFT C_{2v}(anharm)	DFT C_{2v}(harm)	Ref. 17 scaled[a]	description
A_1	1	2935	2968	3039	2950	3084	2946	3050	2914	β-CH_2 sym str.
	2	2873	2924	3059	2973	3102	2943	3074	2933	α-CH_2 sym str. (ip)
	3	2145	2131	2194	2177	2259	2138	2191	2130	SiH_2 sym. str.
	4	1422	1427	1468	1431	1473	1427	1460	1443	α-CH_2 deform. (ip)
	5	1458	1459	1502	1512	1514	1460	1497	1476	β-CH_2 deform.
	6	1127	1130	1158	1133	1166	1130	1154	1141	α-CH_2 wag (ip)
	7	962	960	969	976	994	941	971	952	SiH_2 deform.
	8	877	867	885	881	901	865	885	873	C-C sym. str.
	9	817	809	830	833	851	763	773	819	Si-C sym. str.
	10	532	531	540	550	560	499	508	531	ring deform.
A_2	11	2992	2975	3120	3039	3182	2961	3115	2992	α-CH_2 antisym str. (op)
	12		970	985	973	989	973	992	969	α-CH_2 twist (op)
	13	1211	1220	1251	1224	1259	1220	1257	1232	β-CH_2 twist
	14	736	735	750	738	747	749	763	737	α-CH_2 rock (ip)
	15	514	508	516	518	523	492	493	508	SiH_2 twist
B_2	16	2888	2930	3060	2975	3102	2940	3071	2935	α-CH_2 sym str. (op)
	17	1401	1430	1451	1413	1451	1420	1451	1426	α-CH_2 deform. (op)
	18		1070	1091	1058	1086	1096	1118	1074	α-CH_2 wag (op)
	19	1255	1258	1297	1269	1306	1257	1290	1277	β-CH_2 wag
	20	927	914	940	931	956	921	947	928	C-C antisym. str.

	21	653	633	641	642	651	639	648	633	Si-C antisym. str.
	22	814	801	818	822	835	793	815	803	SiH_2 wag
B_1	23	2953	2933	3080	2997	3140	2942	3084	2954	β-CH_2 antisym str.
	24	2992	2983	3121	3039	3183	2970	3122	2994	α-CH_2 antisym str. (ip)
	25	2145	2140	2202	2183	2266	2143	2197	2138	SiH_2 antisym. Str.
	26	1191	1193	1220	1201	1232	1184	1210	1202	α-CH_2 twist (ip)
	27	906	904	921	918	937	876	893	908	α-CH_2 rock (ip)
	28	673	673	675	670	676	713	712	665	β-CH_2 rock
	29	409	430	416	413	410	440	436	409	SiH_2 rock
	30	158	142	146	184	195	-107	-109	147	ring puckering

[a] Harmonic frequency calculations at C_s symmetry followed by application of empirical scaling factor not given in Ref 17.

Table 2: Quantum numbers of energy levels included in the spectral analysis of the ground state, ν_{29} and ν_{30} bands of SCB.

	0^{+} [a]	0^{-} [a]	$0^{+} \rightarrow \nu_{30}^{+}$	$0^{-} \rightarrow \nu_{30}^{-}$	$0^{+} \rightarrow \nu_{29}^{+}$	$0^{-} \rightarrow \nu_{29}^{-}$	$0^{+} \rightarrow \nu_{29}^{-}$	$0^{-} \rightarrow \nu_{29}^{+}$
type			*c*	*c*	*c*	*c*	*a*	*a*
J(min)	9	5	8	5	4	4	5	4
J(max)	40	52	35	40	45	40	50	52
K_a(min)	0	0	6	0	0	0	0	0
K_a(max)	40	40	35	40	45	40	25	19
K_c(min)	0	0	0	0	0	0	0	0
K_c(max)	33	52	13	30	30	37	50	52
# transitions	763	1108	584	1213	1674	1707	1505	1572

[a] From ground state combination differences.

Table 3: Spectroscopic constants for the ground state, ν_{29} and ν_{30} bands of SCB determined in the present study.

	0^{+} [a]	0^{-} [a]	ν_{30}^{+}	ν_{30}^{-}	ν_{29}^{+}	ν_{29}^{-}
E / cm^{-1}	0	0.002665(6)[b]	158.121851(8)	158.387335(8)	410.037649(15)	410.211480(16)
Rotational constants / cm^{-1}						
A	0.2940600(3)	0.2940595(3)	0.29364182(12)	0.29364649(6)	0.29394943(3)	0.29393379(4)
B	0.2097761(16)	0.2097752(6)	0.2094887(21)	0.20946030(14)	0.20990084(6)	0.20990206(6)
C	0.1416064(7)	0.1416076(3)	0.140842(5)	0.1409270(3)	0.14136853(3)	0.14136597(3)
Centrifugal distortion constants / 10^{-9} cm^{-1}						
Δ_J	79.1(9)	79.8(4)	84.6(4)	81.64(16)	78.645(26)	78.65(3)
Δ_K	207(3)	208.2(13)	222.0(10)	216.6(7)	205.30(8)	206.61(9)
Δ_{JK}	-115(4)	-117.0(17)	-137.1(14)	-129.1(8)	-112.96(10)	-115.00(10)
δ_J	20.4(5)	20.55(19)	20.03[c]	20.03(13)	20.510(14)	21.093(16)
δ_K	51(3)	50.4(8)	67.9[c]	67.9(10)	48.96(6)	52.30(7)
rms error / cm^{-1}	0.000166	0.000198	0.000158			

[a] From ground state combination differences.
[b] From IR global fit.
[c] Fixed to value from ν_{30}^{-} state.

Table 4: Comparison of ground state spectroscopic constants of SCB determined by both pure rotational and rovibrational studies.

	microwave (Ref. 16)		microwave[b] (re-fit in this work)		far infrared (this work)	
	0^+	0^-	0^+	0^-	0^+	0^-
A / cm^{-1}	0.29405982 (6)	0.29405992 (6)	0.29405997(20)	0.29405966(20)	0.2940600 (3)	0.2940595 (3)
B	0.20977825 (7)	0.20977812 (5)	0.20977896(18)	0.20977806(18)	0.2097760 (16)	0.2097752 (6)
C	0.14160694 (8)	0.14160734 (5)	0.14160610(18)	0.14160732(18)	0.1416060 (7)	0.1416076 (3)
Δ_J / 10^{-9} cm^{-1}	70(6)	70[a]	70(23)	70[a]	79.0(9)	79.8(4)
Δ_K	138(7)	138	215(18)	215	207(3)	208.2(14)
Δ_{JK}	-64(7)	-64	-122(20)	-122	-115(4)	-117.0(17)
δ_J	10.5(9)	10.5	20.55[b]	20.55[b]	20.4(5)	20.55(19)
δ_K	-46(10)	-46	50.4	50.4	51(3)	50.4(8)
ΔE /cm^{-1}	0.00252595(9)		0.0025265(3)		0.002665(6)	
# transitions	26		26		763	1108

[a] The centrifugal distortion constants of state 0^- were fixed to those of state 0^+ during the fit in Ref. 16.

[b] The δ_J and δ_K constants were fixed at the values determined from the far infrared analysis.

Figure 1: Potential energy function along the ring puckering coordinate of SCB. The energy levels are not to scale. The barrier to planarity is from ref. 9; the inversion splitting values from ref. 10. The SCB ring is shown in the ac-plane to emphasize the changing angle along the ring puckering coordinate. From this view, the rear CH_2 group is obscured.

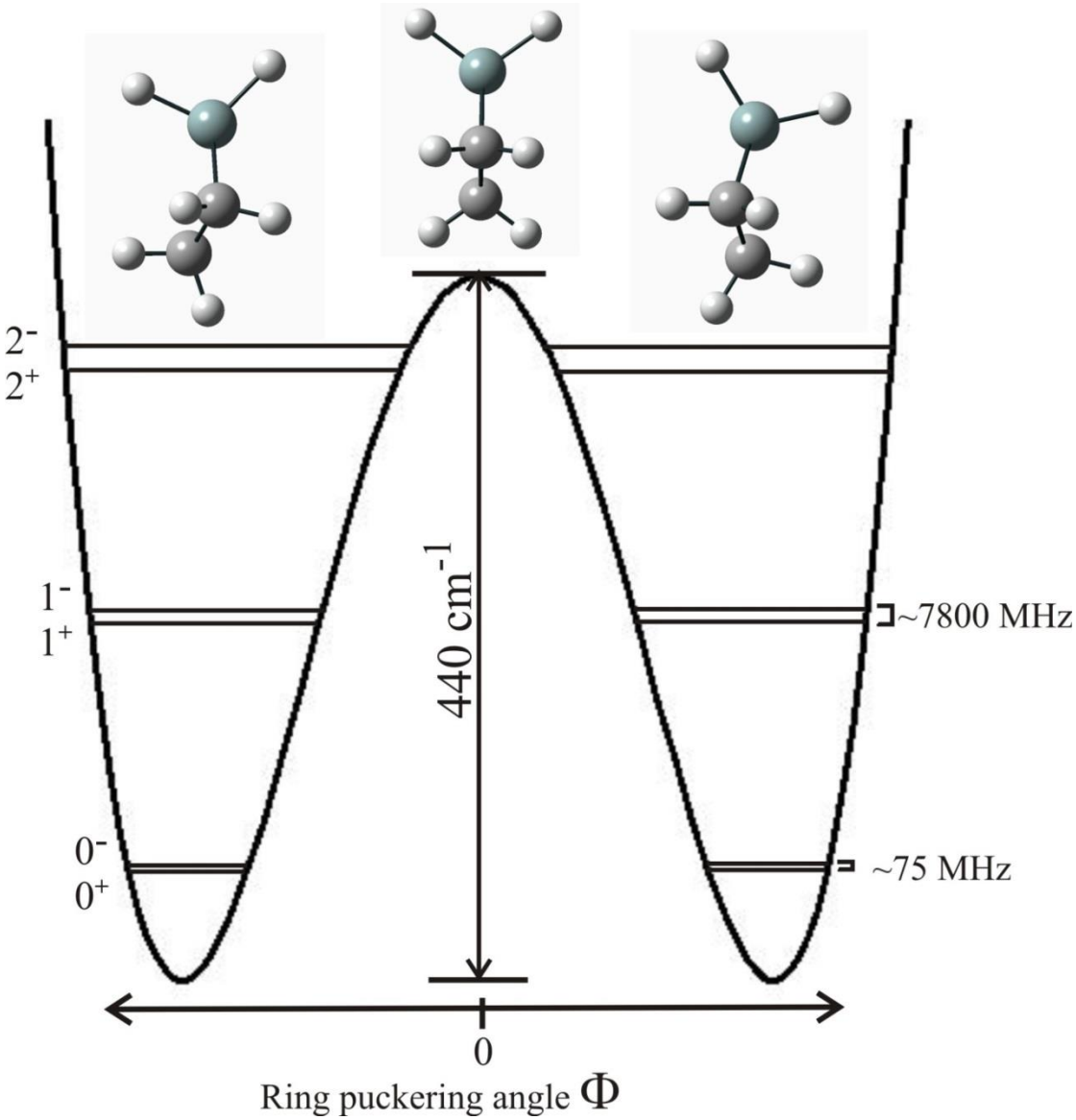

Figure 2: Ground state geometry of SCB in its principal inertial axis system.

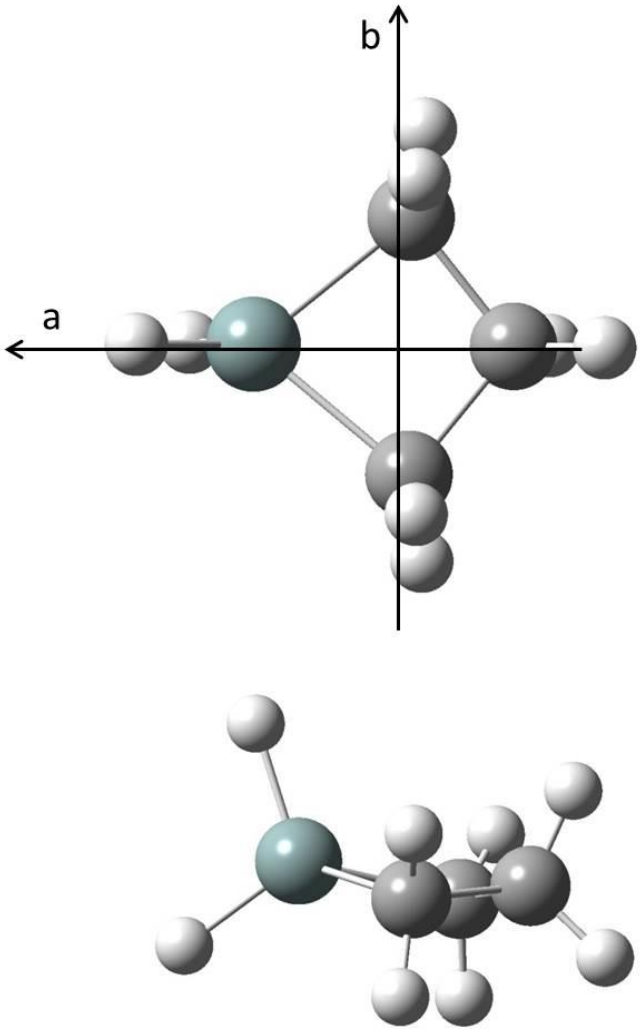

Figure 3: A schematic showing the allowed transitions for the ν_{29} and ν_{30} bands of SCB using the C_{2v} molecular symmetry group. The labels 0/1 denote the ground state and excited vibrational states. The labels +/- denote the ring inversion symmetry of the states. The rotational sub-levels (K_aK_c)(even/odd) are labelled with their rotation-vibration-inversion symmetry.

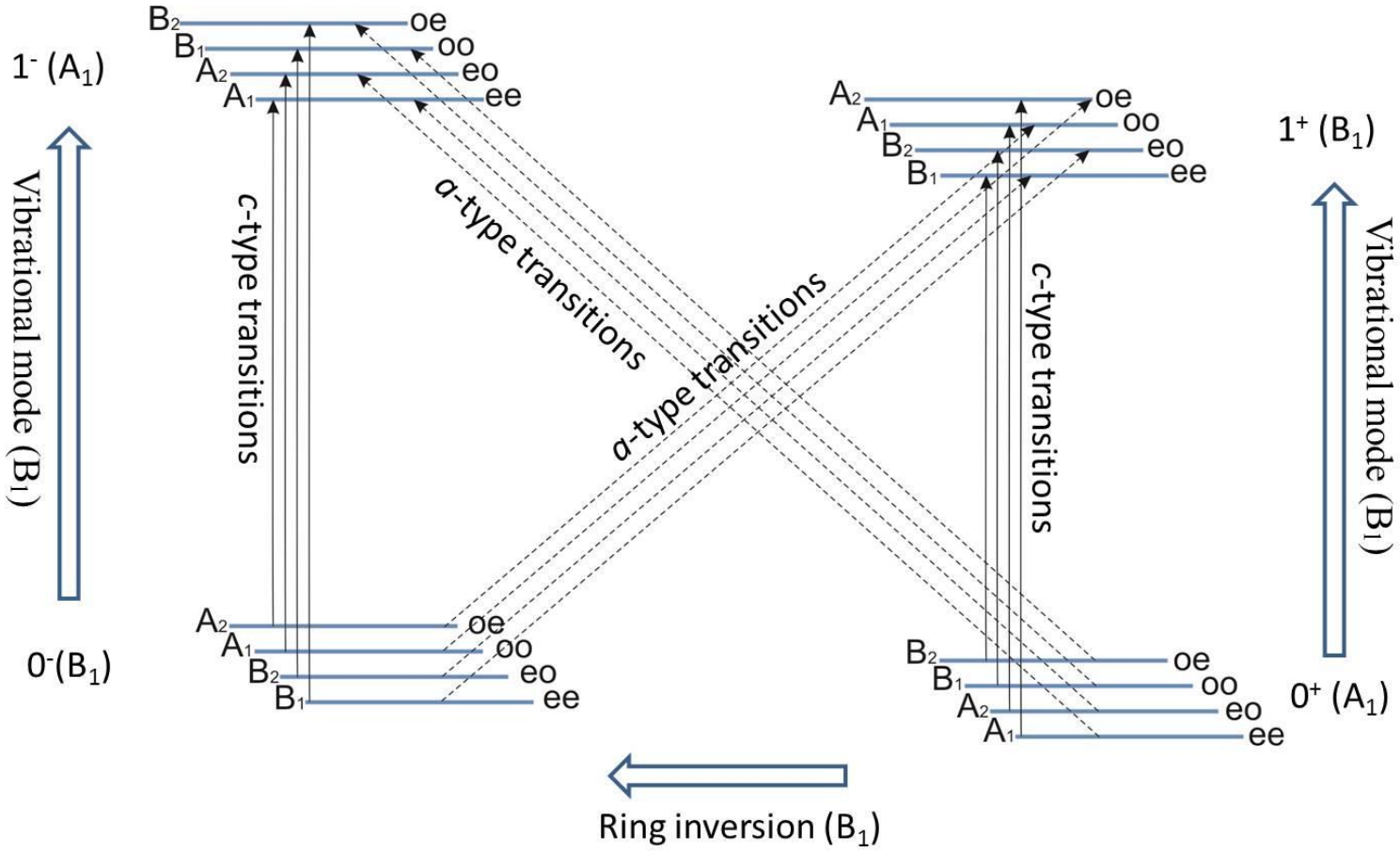

Figure 4: Overview spectrum showing band structure of the ν_{29} SiH_2 rocking band of SCB at ~410 cm^{-1}.

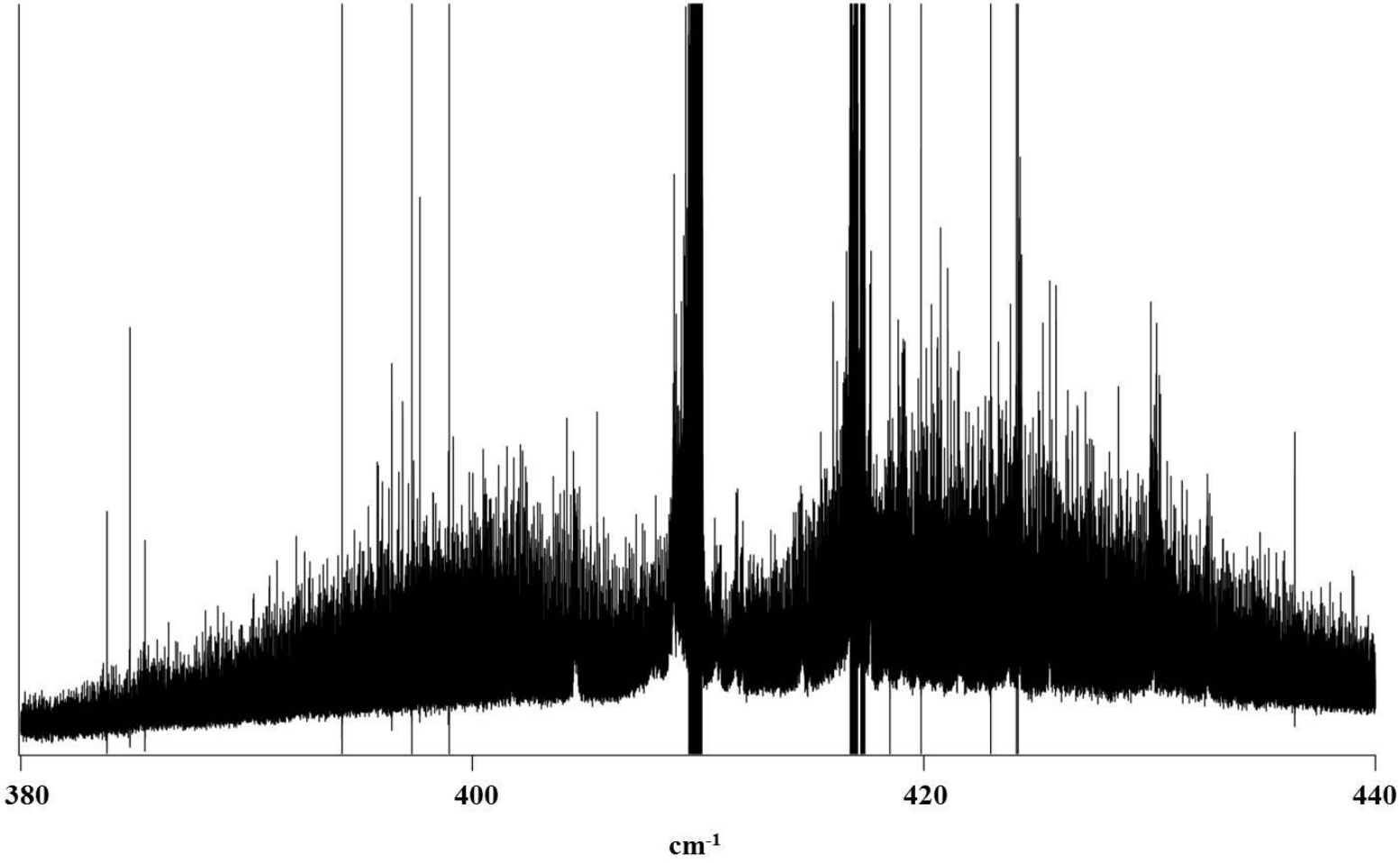

Figure 5: A portion of the Loomis-Wood plot of the ν_{29} band of SCB between ~388 and ~402 cm^{-1} showing *c*-type progressions used to aid in its assignment. The black and green colouring identifies transitions sharing common K_c but having different J values with $0^+ \rightarrow \nu_{29}^+$ and $0^- \rightarrow \nu_{29}^-$, respectively.

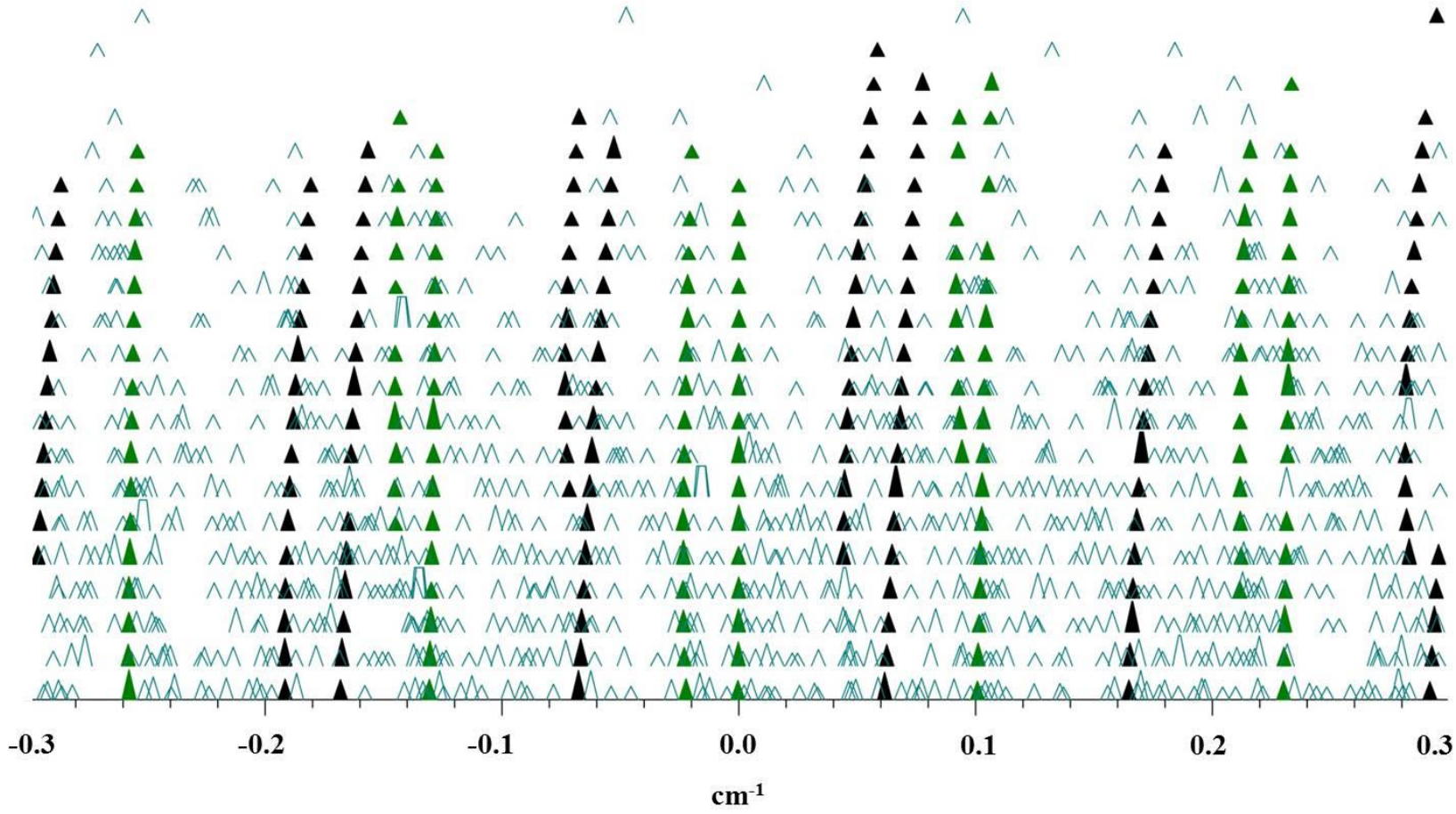

Figure 6: A portion of the Loomis-Wood plot of the ν_{29} band of SCB between ~395 and ~402 cm^{-1} showing *a*-type progressions used to aid in its assignment. The red and blue labels indicate transitions sharing common K_a but having different J values with $0^+ \rightarrow \nu_{29}^-$ and $0^- \rightarrow \nu_{29}^+$, respectively. The rectangle designates the portion of the spectrum shown in Figure 7.

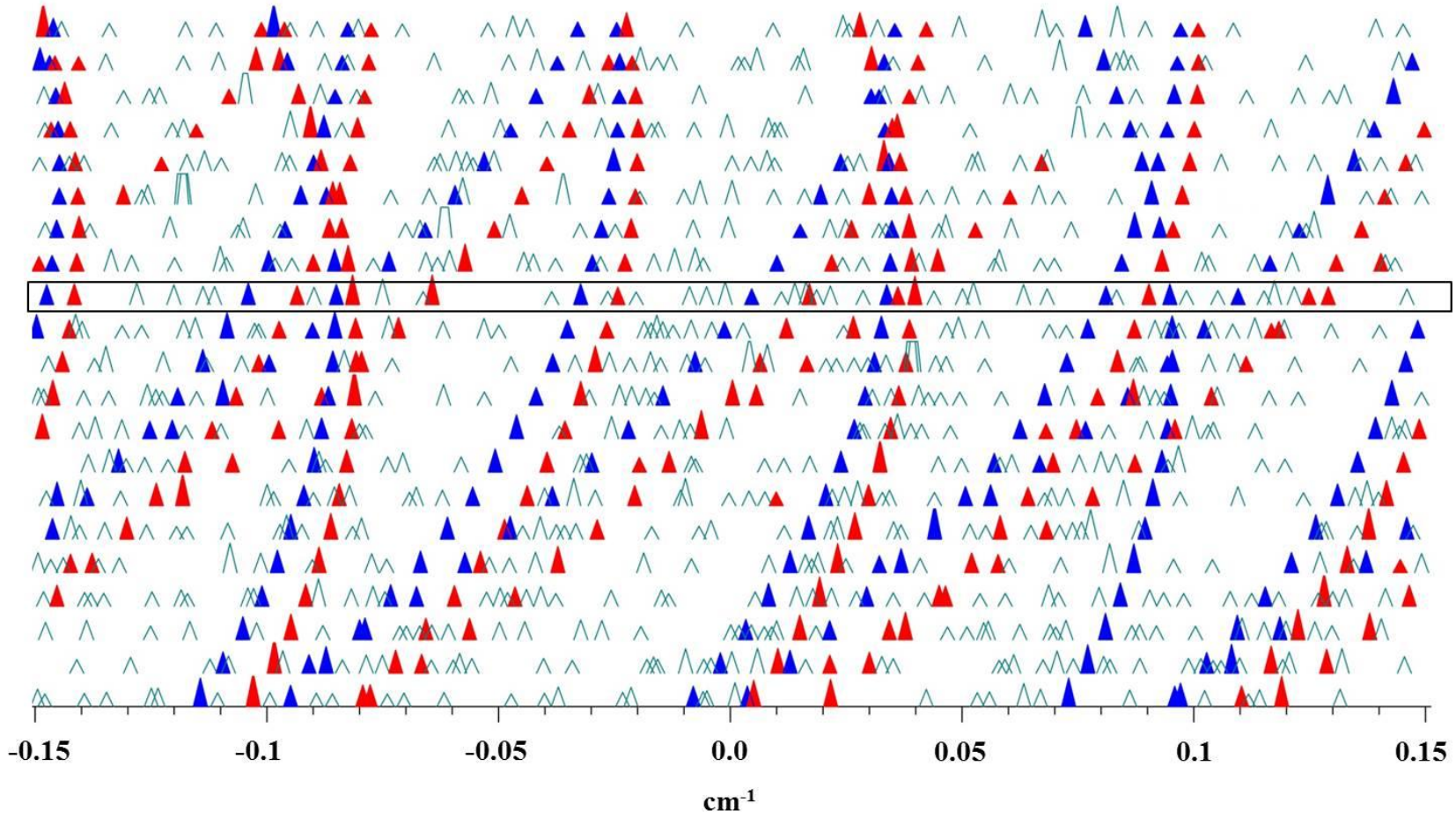

Figure 7: A closer look at a 0.6 cm^{-1} spectral region of the P branch of the ν_{29} band of SCB showing the *a*-type rotation-vibration-inversion transitions that correspond to the box in the Loomis-Wood plot in Figure 6. The *c*-type rotation-vibration transitions are left unlabelled here to avoid congestion.

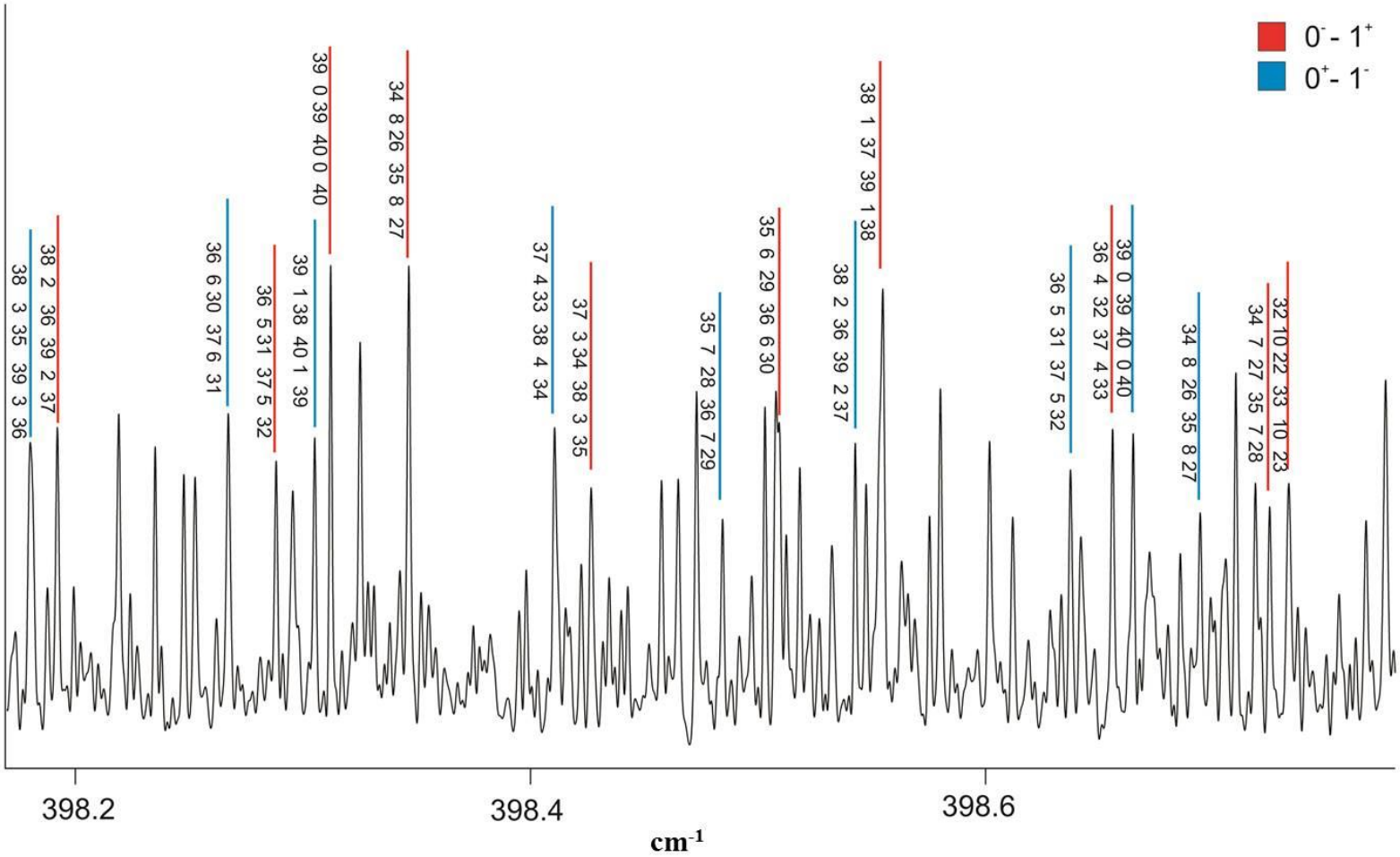

Figure 8: Overview spectrum showing band structure of the ν_{30} ring puckering vibration of SCB at ~158 cm^{-1}.

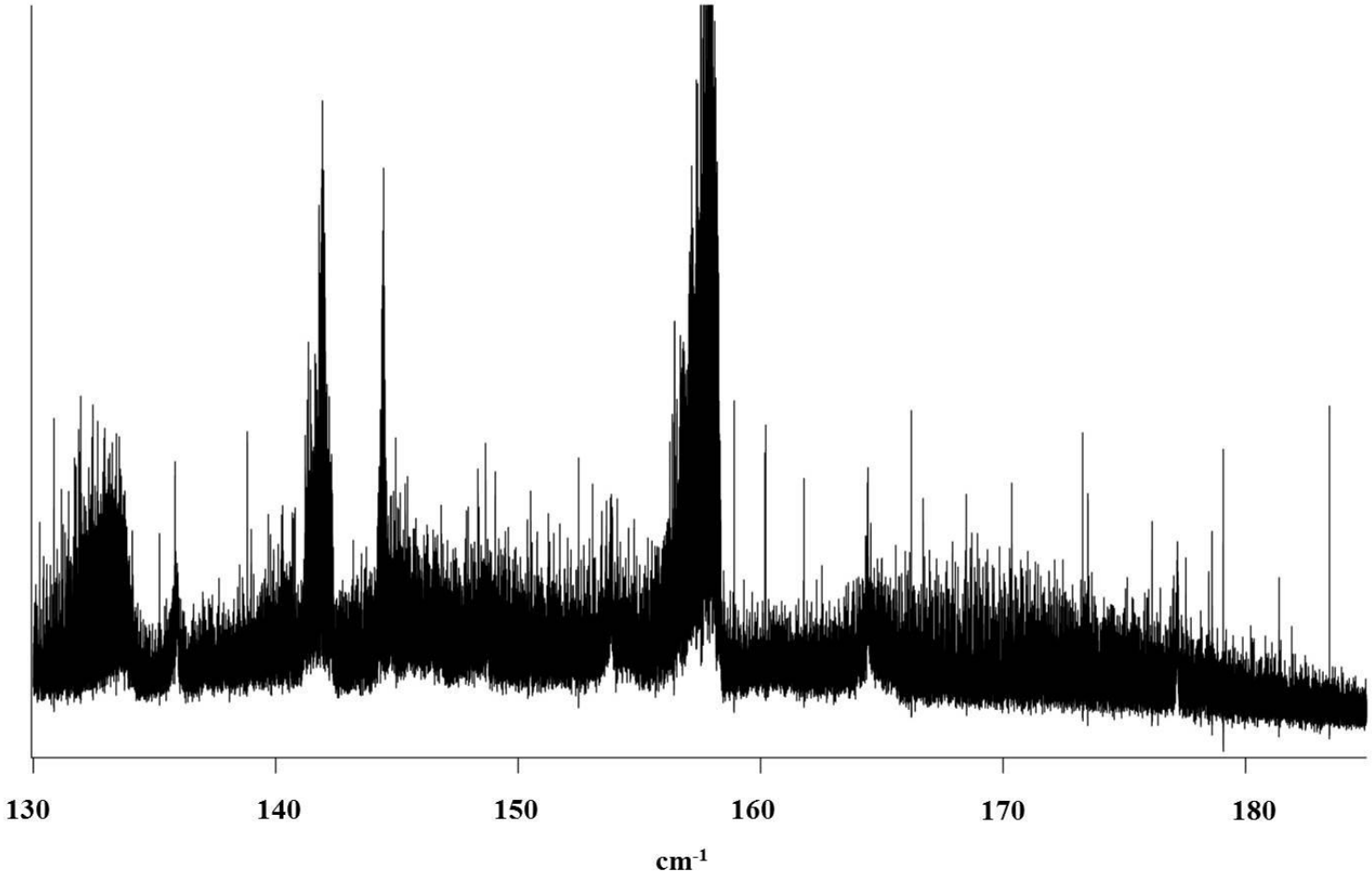

Figure 9: A portion of the Loomis-Wood plot of the ν_{30} band of SCB between ~165 and ~176 cm^{-1} showing *c*-type progressions used to aid in its assignment. . The black and green colouring identifies transitions sharing common K_c but having different J values $0^+ \rightarrow \nu_{30}^+$ and $0^- \rightarrow \nu_{30}^-$, respectively.

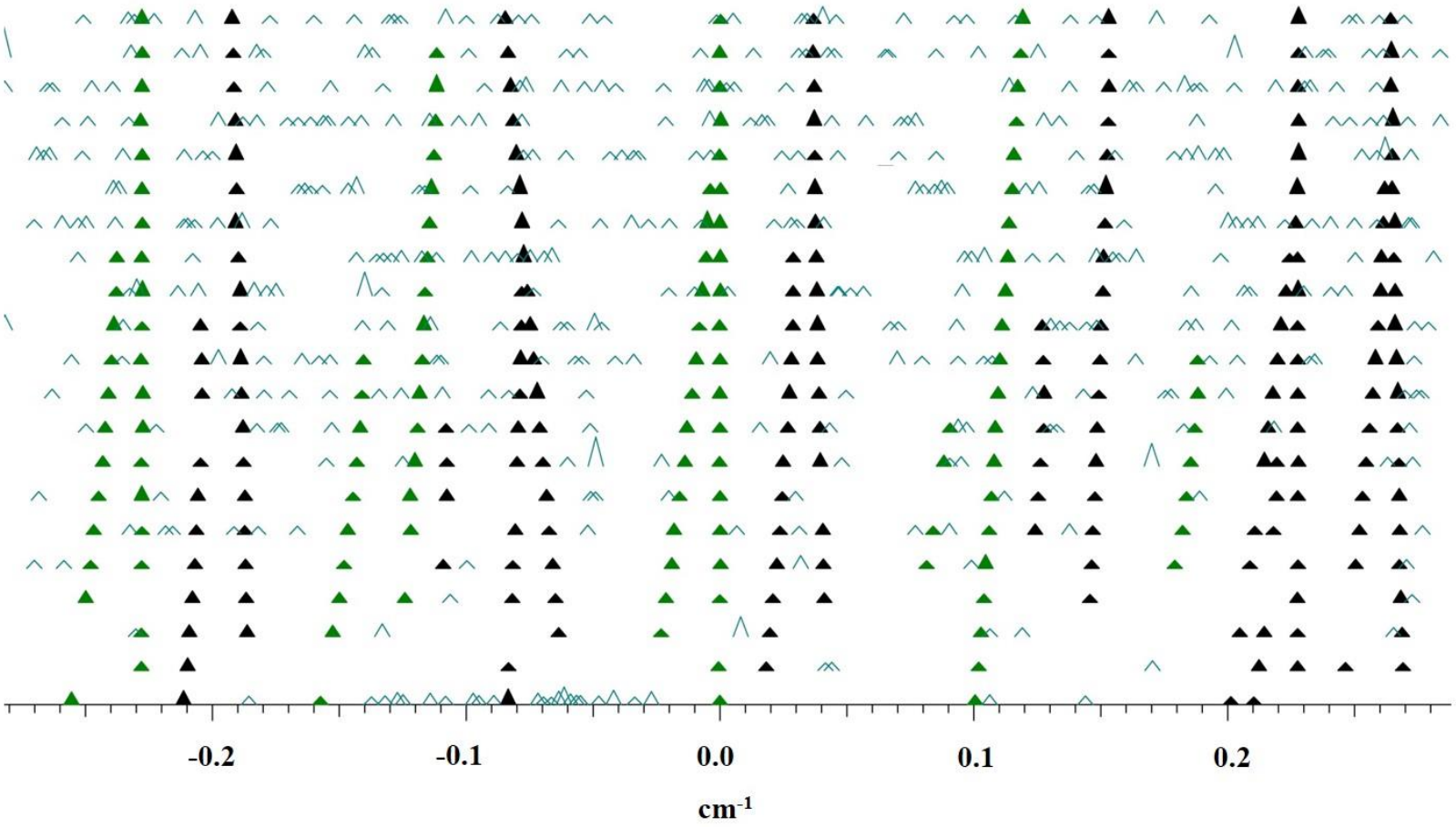

References

[1] I. Badran, T. D. Forster, R. Roesler and Y. J. Shi, J. Phys. Chem A. **116**, 10054-10062 (2012).

[2] V. G. Avakyan, S. S. Bukalov, R. R. Aysin and L. A. Leites, Organometallics. **31**, 7063-7073 (2012).

[3]Z. J. Cai and Y. J. Shi, J. Mol. Spectrosc. **267**, 178-185 (2011).

[4] L. Tong and Y. J. Shi, J. Mass Spectrom. **45**, 215-222 (2010).

[5] Y. J. Shi, B. Lo, L. Tong, X. Li, B. D. Eustergerling and T. S. Sorensen, J. Mass Spectrom. **42**, 575-583 (2007).

[6]T. B. Malloy, J. Mol. Spectrosc. **44**, 504–535 (1972).

[7]A. C. Legon, Chem. Rev. **80**, 231-262 (1980).

[8]J. Laane, Int. Rev. Phys. Chem. **18**, 301–341 (1999).

[9]J. Laane and R. C. Lord, J. Chem. Phys. **48**, 1508-1513 (1968).

[10]W. C. P. Pringle, J. Chem. Phys. **54**, 4979-4988 (1971).

[11]A. Danti, W. J. Lafferty and R. C. Lord, J. Chem. Phys. **33**, 294-295 (1960).

[12]S. I. Chan, T. R. Borgers, J. W. Russell, H. L. Strauss and W. D. Gwinn, J. Chem. Phys. **44**, 1103-1111 (1966).

[13]J. Jokisaari and J. Kauppinen, J. Chem. Phys. **59**, 2260-2263 (1973).

[14]M. Winnewisser, M. Kunzmann, M. Lock and B. P. Winnewisser, J. Mol. Struct. **561**, 1–15 (2001).

[15] G. Moruzzi, M. Kunzmann, B. P. Winnewisser, M. Winnewisser, J. Mol. Spectrosc. **219**, 152–162 (2003).

[16] J. van Wijngaarden, Z. Chen, C. W. van Dijk and J. L. Sorenson, J. Phys. Chem A. **115**, 8650-8655 (2011).

[17] A. A. Al-Saadi and J. Laane, Organometallics, **27**, 3435-3443 (2008).

[18] V. P. Novikov, M. Dakkouri, and L. V. Vilkov, J. Mol. Struct. **800**, 146-153 (2006).

[19]A. R. W. McKellar, J. Mol. Spectrosc. **262**, 1-10 (2010).

[20] J. Laane, J. Am. Chem. Soc. **89**, 1144-1147 (1967).

[21] J. Laane, Spectrochim. Acta. **26A**, 517-540 (1970).

[22] Z. Chen and J. van Wijngaarden, J. Mol. Spectrosc. **268**, 107-111 (2011).

[23] L. S. Rothman, I. E. Gordon, A. Barbe, D. Chris Benner, P. F. Bernath, M. Birk, V. Boudon, L. R. Brown, A. Campargue, J. -P. Champion, K. Chance, L. H. Coudert, V. Danaj, V. M. Devi, S. Fally, J. -M. Flaud, R. R. Gamache, A. Goldmanm, D. Jacquemart, I. Kleiner, N. Lacome, W. J. Lafferty, J. -Y. Mandin, S. T. Massie, S. N. Mikhailenko, C. E. Miller, N. Moazzen-Ahmadi, O. V. Naumenko, A. V. Nikitin, J. Orphal, V. I. Perevalov, A. Perrin, A. Predoi-Cross, C. P. Rinsland, M. Rotger, M. Šimečková, M. A. H. Smith, K. Sung, S. A. Tashkun, J. Tennyson, R. A. Toth, A. C. Vandaele, J. Vander Auwera, J. Quant. Spectrosc. Radiat. Trans. **110**, 533-572 (2009).

[24] H. M. Pickett, R. L. Poynter, E. A. Cohen, M. L. Delitsky, J. C. Pearson, and H. S. P. Muller, J. Quant. Spectrosc. & Rad. Trans. **60,** 883-890 (1998).

[25] Gaussian 03, Revision C.02, M. J. Frisch, G. W. Trucks, H. B. Schlegel, G. E. Scuseria, M. A. Robb, J. R. Cheeseman, J. A. Montgomery, Jr., T. Vreven, K. N. Kudin, J. C. Burant, J. M. Millam, S. S. Iyengar, J. Tomasi, V. Barone, B. Mennucci, M. Cossi, G. Scalmani, N. Rega, G. A. Petersson, H. Nakatsuji, M. Hada, M. Ehara, K. Toyota, R. Fukuda, J. Hasegawa, M. Ishida, T. Nakajima, Y. Honda, O. Kitao, H. Nakai, M. Klene, X. Li, J. E. Knox, H. P. Hratchian, J. B. Cross, V. Bakken, C. Adamo, J. Jaramillo, R. Gomperts, R. E. Stratmann, O. Yazyev, A. J. Austin, R. Cammi, C. Pomelli, J. W. Ochterski, P. Y. Ayala, K. Morokuma, G. A. Voth, P.

Salvador, J. J. Dannenberg, V. G. Zakrzewski, S. Dapprich, A. D. Daniels, M. C. Strain, O. Farkas, D. K. Malick, A. D. Rabuck, K. Raghavachari, J. B. Foresman, J. V. Ortiz, Q. Cui, A. G. Baboul, S. Clifford, J. Cioslowski, B. B. Stefanov, G. Liu, A. Liashenko, P. Piskorz, I. Komaromi, R. L. Martin, D. J. Fox, T. Keith, M. A. Al-Laham, C. Y. Peng, A. Nanayakkara, M. Challacombe, P. M. W. Gill, B. Johnson, W. Chen, M. W. Wong, C. Gonzalez, and J. A. Pople, Gaussian, Inc., Wallingford CT, (2004).

[26] Z. Chen and J. van Wijngaarden, J. Mol. Spectrosc. **257**, 164-169 (2009).

[27] H. M. Pickett, J. Mol. Spectrosc. **148**, 371-377 (1991).

[28] Neese, C. F. Loomis-Wood Add-In (LWA) for Igor Pro, Version 2.0; 56th Ohio State University International Symposium on Molecular Spectroscopy, Columbus, OH, (2005) http://fermi.uchicago.edu/freeware/LoomisWood.shtml.

[29] IGOR Pro, WaveMetric Inc., Lake Oswego, OR USA (2008).

[30] See Supplementary Material Document No._____ for a complete list of assigned transitions. For information on Supplementary Material, see http://www.aip.org/pubservs/epaps.html.